Cell Stem Cell
Article

# Lymphomyeloid Contribution of an Immune-Restricted Progenitor Emerging Prior to Definitive Hematopoietic Stem Cells

Charlotta Böiers,[1,2] Joana Carrelha,[3] Michael Lutteropp,[3] Sidinh Luc,[3] Joanna C.A. Green,[3] Emanuele Azzoni,[4] Petter S. Woll,[3] Adam J. Mead,[3] Anne Hultquist,[1] Gemma Swiers,[4] Elisa Gomez Perdiguero,[5] Iain C. Macaulay,[3] Luca Melchiori,[3] Tiago C. Luis,[3] Shabnam Kharazi,[1] Tiphaine Bouriez-Jones,[3] Qiaolin Deng,[6] Annica Pontén,[7] Deborah Atkinson,[3] Christina T. Jensen,[3] Ewa Sitnicka,[1] Frederic Geissmann,[5] Isabelle Godin,[8] Rickard Sandberg,[6] Marella F.T.R. de Bruijn,[4] and Sten Eirik W. Jacobsen[3,4,9,*]

[1]Haematopoietic Stem Cell Laboratory, Lund Stem Cell Center, Lund University, 221 84 Lund, Sweden
[2]Molecular Medicine and Gene Therapy, Lund Stem Cell Center, Lund University, 221 84 Lund, Sweden
[3]Haematopoietic Stem Cell Laboratory, Weatherall Institute of Molecular Medicine, John Radcliffe Hospital, University of Oxford, Headington, Oxford OX3 9DS, UK
[4]MRC Molecular Haematology Unit, Weatherall Institute of Molecular Medicine, John Radcliffe Hospital, University of Oxford, Headington, Oxford OX3 9DS, UK
[5]Center for Molecular and Cellular Biology of Inflammation, Division of Immunology Infection & Inflammatory Diseases, King's College London, London SE1 1UL, UK
[6]Department of Cell and Molecular Biology, Karolinska Institutet and Ludwig Institute for Cancer Research, 171 77 Stockholm, Sweden
[7]Cardiovascular group, Lund Stem Cell Center, Lund University, 221 84 Lund, Sweden
[8]Institut National de la Santé et de la Recherche Médicale, INSERM 1009, Université Paris-Sud, Orsay, 94805 Villejuif, France
[9]Department of Cell and Molecular Biology, Wallenberg Institute for Regenerative Medicine and Department of Medicine, Center for Hematology and Regenerative Medicine, Karolinska Institutet, 171 77 Stockholm, Sweden
*Correspondence: sten.jacobsen@imm.ox.ac.uk
http://dx.doi.org/10.1016/j.stem.2013.08.012

## SUMMARY

**In jawed vertebrates, development of an adaptive immune-system is essential for protection of the born organism against otherwise life-threatening pathogens. Myeloid cells of the innate immune system are formed early in development, whereas lymphopoiesis has been suggested to initiate much later, following emergence of definitive hematopoietic stem cells (HSCs). Herein, we demonstrate that the embryonic lymphoid commitment process initiates earlier than previously appreciated, prior to emergence of definitive HSCs, through establishment of a previously unrecognized entirely immune-restricted and lymphoid-primed progenitor. Notably, this immune-restricted progenitor appears to first emerge in the yolk sac and contributes physiologically to the establishment of lymphoid and some myeloid components of the immune-system, establishing the lymphomyeloid lineage restriction process as an early and physiologically important lineage-commitment step in mammalian hematopoiesis.**

## INTRODUCTION

The mammalian hematopoietic system is considered the paradigmatic and best-understood model for how multilineage diversity is achieved by stepwise lineage restriction of a multipotent stem cell (Orkin and Zon, 2008a). Although multipotent hematopoietic stem cells (HSCs) possessing all blood-lineage potentials have been unequivocally established to reside at the top of the hematopoietic hierarchy (Osawa et al., 1996), the exact roadmap for hematopoietic lineage restriction remains disputed, in particular with regard to the first lineage-restriction steps of HSCs (Orkin and Zon, 2008a; Schlenner and Rodewald, 2010; Ye and Graf, 2007). The classical hematopoietic hierarchy still prevailing in textbooks predicts that the first lineage-restriction decision made by adult HSCs results in strictly separated pathways for the lymphoid and myeloerythroid lineages (Orkin and Zon, 2008b; Seita and Weissman, 2010) as supported by the identification of common lymphoid (Kondo et al., 1997) and common myeloid (Akashi et al., 2000; Arinobu et al., 2007) progenitors (CLPs and CMPs, respectively).

However, earlier in vitro findings demonstrating that clonal lineage outputs of heterogeneous fetal hematopoietic progenitors excluded combined B and T cell generation in the absence of myeloid cells, challenged the classical hematopoietic hierarchy, and led to the proposal that the first lineage decisions of HSCs might rather result in a separation into a CMP and a lymphomyeloid progenitor pathway (Katsura and Kawamoto, 2001), a hypothesis supported by additional studies (Cumano et al., 1992; Lacaud et al., 1998). More recently, lymphoid-primed multipotent progenitors (LMPPs) were prospectively isolated and shown at the single-cell level to possess combined granulocyte-macrophage (GM) and B and T lymphocyte potential but little or no megakaryocyte-erythroid (MkE) potential (Adolfsson et al., 2005; Månsson et al., 2007), providing direct evidence for the existence of a lymphomyeloid-restricted pathway in mammalian hematopoiesis. However, the revised

hematopoietic hierarchy has been challenged by studies implying that LMPPs possess considerable MkE potential in vivo (Boyer et al., 2011; Forsberg et al., 2006). Thus, whether the first lineage fate decision of multipotent stem-progenitor cells results in establishment of completely separated pathways of the myeloid and lymphoid components of the immune system or a common lymphomyeloid immune pathway remains unresolved (Boyer et al., 2012; Orkin and Zon, 2008a; Schlenner and Rodewald, 2010; Seita and Weissman, 2010; Ye and Graf, 2007). Moreover, the in vivo physiological relevance of the lymphomyeloid pathway has been challenged based on in vivo fate mapping studies concluding that adult lymphomyeloid-restricted progenitors contribute almost exclusively to lymphopoiesis and not myelopoiesis (Boyer et al., 2011; Schlenner et al., 2010; Welner et al., 2009).

Lineage-fate decisions of multipotent stem and progenitor cells take place for the first time during early embryonic development. Blood cells appear in the mouse embryo at embryonic day (E) 7 in the yolk sac (YS). This first wave of primitive hematopoiesis is myeloerythroid-restricted and transient (Medvinsky et al., 2011). In addition, resident tissue macrophages, such as brain microglia, liver Kupffer cells, and epidermal Langerhans cells, develop between E8.5 and E9.5 independently of definitive HSCs (Schulz et al., 2012). The first definitive multipotent HSCs, defined as cells capable of long-term repopulation of all myeloerythroid and lymphoid lineages in adult recipient mice are not found until after E10.5 (Medvinsky and Dzierzak, 1996). These HSCs, first generated in the aorta-gonad-mesonephros (AGM) region, subsequently at E11 seed the fetal liver (FL), the main fetal hematopoietic site (Kumaravelu et al., 2002; Medvinsky and Dzierzak, 1996). Because the first lymphoid-restricted embryonic progenitors have been identified after definitive HSCs seed the FL (Douagi et al., 2002), it has been assumed that lymphoid lineage restriction does not initiate before the FL is seeded by definitive HSCs. However, there are several findings compatible with lymphoid lineage commitment potentially initiating earlier. Progenitors possessing all myeloerythroid and lymphoid lineage potentials have been identified before emergence of definitive HSCs and FL hematopoiesis (Kieusseian et al., 2012; Rybtsov et al., 2011; Yoshimoto et al., 2012) and at E10.5–E11, low-level expression of interleukin-7 receptor alpha (IL7Rα) and the recombination activating gene 1 (*Rag1*), regulators of early lymphoid development, have been described in the embryo (Kawamoto et al., 2000; Yokota et al., 2006) Although the identity of these early IL7Rα and *Rag1*-expressing cells has not been investigated in detail, they could potentially reflect multilineage transcriptional-primed multipotent progenitors (Hu et al., 1997; Månsson et al., 2007). However, the earliest IL7Rα-expressing progenitors have rather been suggested to be fully B or T lymphocyte-restricted and to lack myeloid lineage potential (Kawamoto et al., 2000), coinciding with or even preceding evidence of lymphomyeloid lineage restriction, suggesting that B and T lymphoid lineage restriction might occur independently of a lymphomyeloid lineage restriction step.

Herein we prospectively identified an IL7Rα-expressing lymphomyeloid-restricted embryonic progenitor as early as E11.5 that sustains combined lymphoid and GM transcriptional lineage priming and potential at the single-cell level but lacks MkE potential. We tracked this lymphomyeloid progenitor back to E9.5 YS, preceding both hematopoietic colonization of the FL and the establishment of definitive HSCs. Through in vivo fate mapping, we confirmed the inability of *Rag1*-expressing early embryonic progenitors to significantly contribute to the MkE lineage while unequivocally and robustly contributing to the myeloid innate, as well as lymphoid adaptive, immune systems of the mammalian embryo. These findings identify the developmentally earliest immune-restricted progenitor and establish the lymphomyeloid restriction as a physiologically important lineage-commitment step in embryonic mammalian hematopoiesis, preceding the emergence of definitive HSCs.

## RESULTS

### Interleukin-7 Receptor Expression Defines Immune-Restricted Embryonic Progenitors with Combined Lymphoid and Granulocyte-Macrophage Lineage Potentials

Expression of IL7Rα has been suggested to be restricted to lymphoid progenitors. We investigated IL7Rα expression in FL at E11.5 and in agreement with previous findings (Kawamoto et al., 2000) we found IL7Rα$^+$ cells coexpressing the pan-hematopoietic marker CD45 and the progenitor cell receptor c-Kit (Kit) but negative for mature lineage markers (Lin$^-$) (Figure 1A). A large fraction of Lin$^-$Kit$^+$IL7Rα$^+$ cells also expressed the myeloid colony-stimulating factor 1 receptor (Csf1r) and the thrombopoietin receptor (ThpoR) (Figure 1A), also expressed by HSCs (Solar et al., 1998). Most IL7Rα$^+$ cells (>70%) coexpressed c-fms-like tyrosine kinase 3 receptor (Flt3) (0.20% of FL cells; Figure 1B), highly expressed on early lymphomyeloid progenitors in adult bone marrow (Adolfsson et al., 2005). Single-cell assays demonstrated that Lin$^-$Kit$^+$Flt3$^+$IL7Rα$^+$ E11.5 FL cells possess considerable GM potential with as many as 43% of single cells forming GM clones, whereas virtually no cells (<1%) possessed Mk or E potential (Figures 1C–1F). Single Lin$^-$Kit$^+$Flt3$^+$IL7Rα$^+$ cells generated 31% and 35% of B and T cell progeny, respectively (Figures 1G and 1H). In vitro cytokine response experiments with the ligands for Flt3 and IL7Rα demonstrated that Flt3 and IL7Rα are expressed at functionally relevant levels on Lin$^-$Kit$^+$Flt3$^+$IL7Rα$^+$ progenitors (see Figure S1A available online). However, in contrast to later emerging B and T lymphoid-restricted progenitors critically dependent on Flt3 and IL7Rα signaling (Sitnicka et al., 2003), investigation of embryos genetically deleted for expression of both Flt3 ligand and the common gamma chain of the IL7R demonstrated that E11.5 Lin$^-$Kit$^+$Flt3$^+$IL7Rα$^+$ progenitors emerge independently of Flt3 and IL7R signaling (Figures S1B and S1C).

Investigation of single Lin$^-$Kit$^+$Flt3$^+$IL7Rα$^+$ E11.5 FL cells demonstrated that more than 70% coexpressed lymphoid (*Il7r*, *Rag1*, and *sIgh)* and GM (*Csf3r* [*Gcsfr*] and *Mpo*), but not the MkE (*Vwf*, *Epor*, and *Gata1*) transcripts typically expressed by multipotent progenitors with MkE potential (Figures 2A and 2B)(Månsson et al., 2007). When compared to Lin$^-$Kit$^+$Flt3$^-$IL7Rα$^-$ cells, the downregulation of MkE-affiliated and upregulation of lymphoid genes expressed prior to B and T cell commitment was further verified through single-cell quantitative gene expression analysis (Figure 2C). Notably,

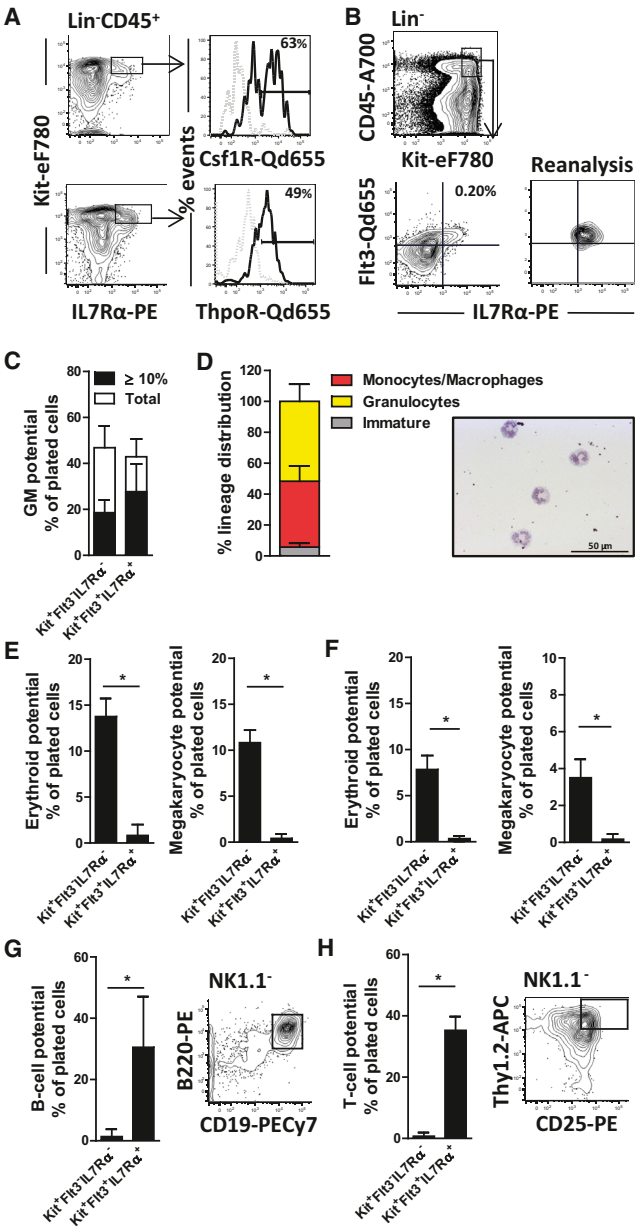


**Figure 1. Interleukin-7-Receptor Expressing Early Fetal Liver Progenitors Have Lymphomyeloid Lineage Potentials**

(A) Coexpression of cell-surface IL7Rα, Csf1R (upper panel) and ThpoR (lower panel) in E11.5 FL Lin$^-$Kit$^+$ progenitors. Viable cells were gated Lin$^-$CD45$^+$. Further gating is indicated in the figure. Grey lines represent negative controls. Mean percentages of Lin$^-$CD45$^+$Kit$^+$IL7Rα$^+$ cells coexpressing Csf1R or ThpoR, respectively, are shown (three experiments).

(B) Lin$^-$Kit$^+$Flt3$^+$IL7Rα$^+$ E11.5 FL cell purification by FACS (purity reanalysis right panel). Mean percentage of total FL cells (>3 experiments) is shown.

(C) GM lineage potential in liquid culture of single Lin$^-$Kit$^+$Flt3$^-$IL7Rα$^-$ and Lin$^-$Kit$^+$Flt3$^+$IL7Rα$^+$ E11.5 FL cells (white bars represent total cloning; black bars represent clones covering ≥ 10% of well; >350 cells per population). Mean ± SD.

(D) Bulk-sorted Lin$^-$Kit$^+$Flt3$^+$IL7Rα$^+$ E11.5 FL cells were cultured under myeloid conditions and evaluated morphologically. Mean ± SD (three biological replicates). Right panel shows representative granulocytes.

(E) Erythroid (left panel) and megakaryocyte (right panel) lineage potential of single Lin$^-$Kit$^+$Flt3$^-$IL7Rα$^-$ and Lin$^-$Kit$^+$Flt3$^+$IL7Rα$^+$ E11.5 FL cells in liquid culture. Mean percentages ± SD (≥450 cells per assay).

this single-cell analysis demonstrated that every Lin$^-$Kit$^+$Flt3$^+$IL7Rα$^+$ progenitor cell expressing these lymphoid genes coexpressed myeloid lineage genes, whereas none of them expressed signature genes of the earliest B (*Pax5*) and T (*Ptcra*) cell restricted progenitors.

Clones derived from single Lin$^-$Kit$^+$Flt3$^+$IL7Rα$^+$ E11.5 FL cells were analyzed for the combined potential for generation of GM, B, and T cells (Figures 2D and 2E). Of the single cell-derived clones that gave a lineage readout, as many as 45% produced mature cells of all three GM, B, and T cell lineages (GM/B/T; Figures 2F and 2G). Natural killer (NK) cells, a third lymphoid lineage and part of the innate immune system, were generated in the majority of the single cell-derived GM/B/T clones (Figure 2H). Virtually no erythroid cells were produced even upon inclusion of erythroid-promoting cytokines (Figure 2I), which stimulated erythropoiesis from the more heterogeneous Lin$^-$Kit$^+$Flt3$^-$IL7Rα$^-$ progenitors (Figures S2A and S2B).

Paired immunoglobulin like receptor (PIR) expression has been shown to separate T and B cell progenitors later in embryonic development. Specifically, in E13.5, FL T cell restricted progenitors were found to coexpress IL7Rα and PIR, whereas B cell progenitors were IL7Rα$^+$PIR$^-$ (Masuda et al., 2005). We found that only a small fraction (11%) of E11.5 FL Lin$^-$Kit$^+$Flt3$^+$IL7Rα$^+$ progenitors expressed cell surface PIR (Figure 2J). The PIR expression was confirmed by quantitative PCR and shown to coincide with upregulation of other early lymphoid transcripts, whereas both PIR$^+$ and PIR$^-$ Lin$^-$Kit$^+$Flt3$^+$IL7Rα$^+$ cells expressed myeloid genes (Figure 2K). In agreement with representing the E11.5 FL lymphomyeloid-restricted progenitors with combined GM, B, and T cell potential, Lin$^-$Kit$^+$Flt3$^+$IL7Rα$^+$PIR$^-$ cells showed robust readout of all three lineage potentials, whereas the small fraction of Lin$^-$Kit$^+$Flt3$^+$IL7Rα$^+$PIR$^+$ cells showed reduced T and undetectable B cell potential (Figure 2L). Thus, at the time of its first seeding by definitive HSCs, the FL contains Lin$^-$Kit$^+$Flt3$^+$IL7Rα$^+$ progenitors with combined lymphomyeloid, but no MkE transcriptional priming or potential.

## Emergence of Immune-Restricted Progenitors Prior to Definitive HSCs

A large number of Lin$^-$Kit$^+$Flt3$^+$IL7Rα$^+$ immune-restricted progenitors (1,200 ± 200 cells/FL) were already present by E11.5. In contrast, we did not detect any long-term multilineage reconstitution activity in E10.5 or E11.5 FL (whether transplanted intravenously or directly into the bones), whereas considerable HSC activity was found in E12.5 FL (Figure 3A; Figures S3A–S3D). These findings are in agreement with previous studies, which suggest that there is at most only one definitive HSC in the FL at E11.5 (Kumaravelu et al., 2002). To enhance the possibility

(F) Erythroid (left panel) and megakaryocyte (right panel) potential of Lin$^-$Kit$^+$Flt3$^+$IL7Rα$^+$ E11.5 FL cells in semisolid medium. Mean percentages ± SD (600 cells, 3 experiments).

(G) B cell (NK1.1$^-$CD19$^+$B220$^+$) and (H) T cell (NK1.1$^-$CD25$^+$Thy1.2$^{hi}$ and/or NK1.1$^-$CD4$^+$CD8$^+$) potential of single Lin$^-$Kit$^+$Flt3$^-$IL7Rα$^-$ and Lin$^-$Kit$^+$Flt3$^+$IL7Rα$^+$ E11.5 FL cells in Op9 and Op9DL1 coculture, respectively. Representative FACS plots. Mean percentages ± SD (≥90 cells per assay), *$p \leq 0.05$.

See also Figure S1.

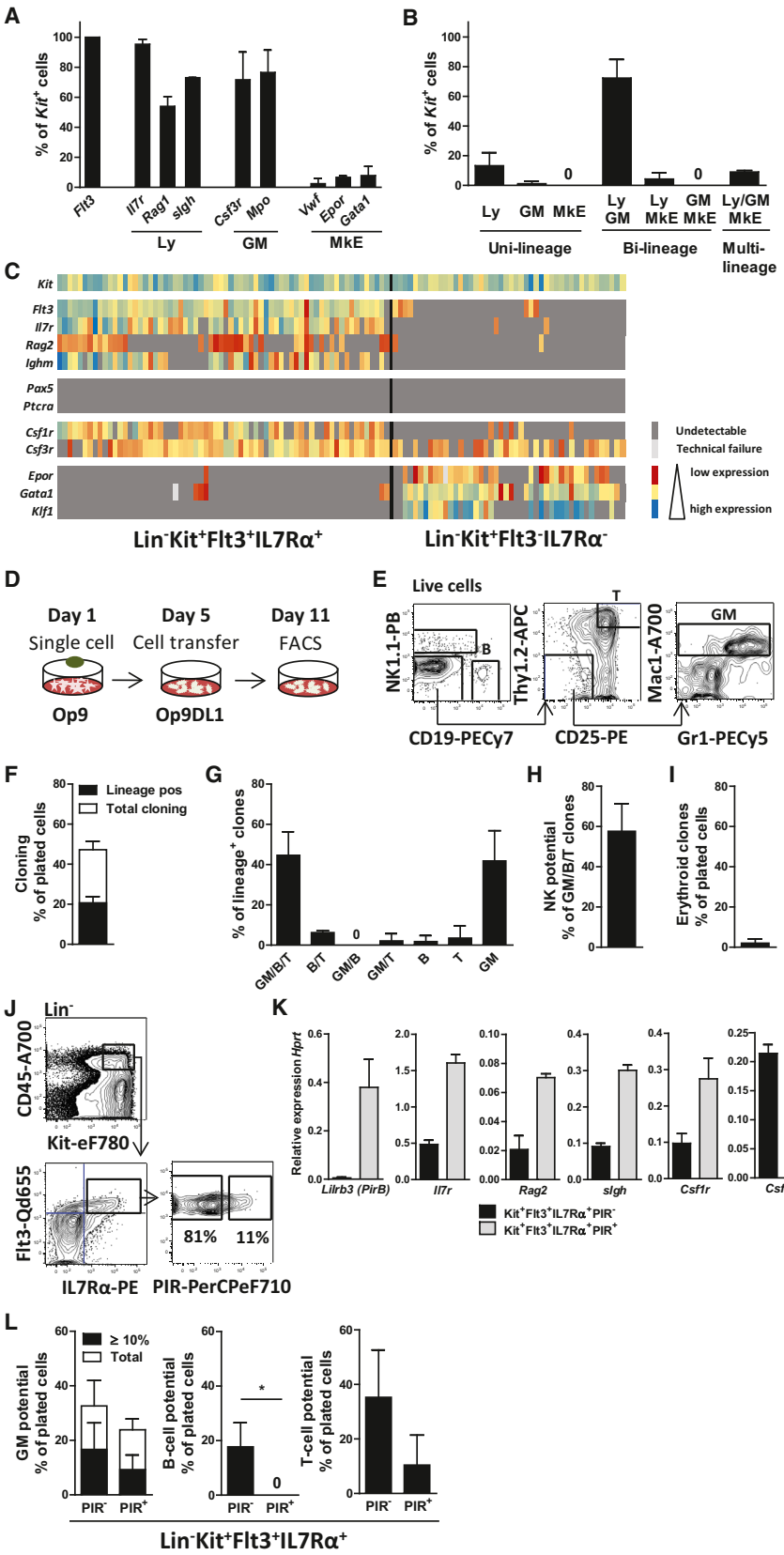


**Figure 2. Combined GM and Lymphoid Transcriptional Priming and Lineage Potentials of Single IL7Rα+ E11.5 Fetal Liver Progenitors**

(A) Single-cell RT-PCR analysis of Lin$^-$Kit$^+$Flt3$^+$IL7Rα$^+$ E11.5 FL cells and (B) combined lineage transcriptional priming patterns based on (A). Mean percentages ± SD of total *Kit*$^+$ cells (>93%; ≥130 cells).

(C) Quantitative gene-expression analysis of single Lin$^-$Kit$^+$Flt3$^+$IL7Rα$^+$ and Lin$^-$Kit$^+$Flt3$^-$IL7Rα$^-$ E11.5 progenitors. Expression of early lymphoid (*Flt3*, *Il7r*, *Rag2*, *Ighm*), B cell-specific (*Pax5*), T cell-specific (*Ptcra*), myeloid (*Csf1r*, *Csf3r*), and MkE (*Epor*, *Gata1*, *Klf1*) related genes were determined as Δ Ct values and normalized to the mean of *Gapdh* and *Hprt*. Each column represents a single cell (≥45 cells per population).

(D) Experimental strategy for establishing combined lineage potentials of Lin$^-$Kit$^+$Flt3$^+$IL7Rα$^+$ E11.5 FL cells. Single cells were deposited directly into wells with Op9 stroma cells. After 5 days of culture, clones were transferred to Op9DL1 stroma cells. Clones were analyzed for lineages after 11 days of culture.

(E) Representative FACS profile of Lin$^-$Kit$^+$Flt3$^+$IL7Rα$^+$ E11.5 FL single-cell-derived GM/B/T clone. A clone was scored positive for B cells if containing NK1.1$^-$CD19$^+$ cells; T cells if NK1.1$^-$CD19$^-$CD25$^+$Thy1.2$^{hi}$ cells and GM cells if containing NK1.1$^-$CD19$^-$CD25$^-$Thy1.2$^-$Mac1$^+$ Gr1$^{-/+}$ cells.

(F) Cloning frequency (white bar; black bar represents clones assigned to the GM, B, and/or T lineage) and (G) lineage (GM/B/T) composition of lineage-positive clones derived from single Lin$^-$Kit$^+$Flt3$^+$IL7Rα$^+$ E11.5 FL cells and (H) frequency of combined GM/B/T clones also containing NK (NK1.1$^+$CD19$^-$CD25$^-$Thy1.2$^-$) cells. Data in (F)–(H) are mean percentages ± SD (≥230 cells investigated).

(I) Frequency of Lin$^-$Kit$^+$Flt3$^+$IL7Rα$^+$ E11.5 FL progenitors with erythroid potential (clones with Ter119$^+$CD71$^+$ cells and/or positive by morphology) on Op9 stroma under conditions promoting erythroid development. Mean percentage ± SD of plated cells (150 cells investigated, 3 experiments).

(J) Lin$^-$Kit$^+$Flt3$^+$IL7Rα$^+$ E11.5 FL progenitors were fractionated based on expression of PIR. Mean percentages within Lin$^-$Kit$^+$Flt3$^+$IL7Rα$^+$ compartment (four experiments).

(K) Quantitative gene expression analysis of lymphoid and myeloid transcripts in Lin$^-$Kit$^+$Flt3$^+$IL7Rα$^+$PIR$^-$ and PIR$^+$ cells. Mean expression ± SD normalized to *Hprt* (2 biological replicates, 25 cells per population).

(L) Lineage potentials of single Lin$^-$Kit$^+$Flt3$^+$IL7Rα$^+$PIR$^-$ and PIR$^+$ cells. GM potential (left panel) (white bars represent total cloning; black bars represent clones covering ≥10% of well), B cell potential (middle panel), and T cell potential (right panel). Mean percentages ± SD; two to three experiments, *p ≤ 0.05.

See also Figure S2.

to identify rare lymphoid-primed progenitors in the early FL, and because expression of Flt3 and *Rag1*-GFP highly overlap in Lin$^-$Kit$^+$Flt3$^+$IL7R$\alpha^+$ E11.5 progenitors (Figure 3B), we used a *Rag1*-GFP reporter to identify a distinct population of Lin$^-$Kit$^+$*Rag1*GFP$^+$IL7R$\alpha^+$ E10.5 FL progenitors (Figure 3C), which possessed GM, B, and T cell, but no MkE potential, as in the E11.5 FL (Figures 3D–3G; Figure S3E), establishing that immune-restricted progenitors are present in the FL already prior to and independently of definitive HSCs.

We next explored how early Lin$^-$Kit$^+$*Rag1*GFP$^+$IL7R$\alpha^+$ lymphomyeloid-primed progenitors emerge in the embryo. In whole E8.5 concepti, virtually no *Rag1*GFP$^+$IL7R$\alpha^+$-positive cells were found, neither in the CD45$^-$ nor in the small CD45$^+$ fraction (Figure 3H). Because the first hematopoietic cells to colonize the FL at E10 might come from the YS, we analyzed YS at E9.5 and observed a small but distinct Lin$^-$Kit$^+$*Rag1*GFP$^+$IL7R$\alpha^+$ cell population (30 ± 4 cells/YS; Figure 3I). Notably, whereas most hematopoietic cells at E9.5 have yet to upregulate expression of the pan-hematopoietic marker CD45, virtually all Lin$^-$Kit$^+$*Rag1*GFP$^+$IL7R$\alpha^+$ cells were CD45$^+$ although most also expressed CD41, and a small fraction the endothelial marker VE-Cadherin (Figure 3J). The placenta and the para-aortic-splanchnopleura (PAS, to become the AGM) region from E9.5 embryos were also investigated, but no *Rag1*GFP$^+$IL7R$\alpha^+$ cells were detected above background level (Figure 3I).

Almost 80% of the rare purified E9.5 YS Lin$^-$Kit$^+$*Rag1*GFP$^+$IL7R$\alpha^+$ cells expressed combined lymphoid GM but no MkE transcriptional priming at the single-cell level (Figures 3K and 3L), similar to E11.5 FL Lin$^-$Kit$^+$Flt3$^+$IL7R$\alpha^+$ cells (Figures 2A–2B), demonstrating that lymphomyeloid-primed progenitors emerge as early as E9.5.

To further investigate the embryonic site of origin of the lymphoid-primed immune-restricted progenitors, whole-mount imaging of *Rag1*GFP$^+$ embryos was performed. In agreement with the fluorescence-activated cell sorting (FACS) analysis, *Rag1*GFP$^+$ cells coexpressing CD45 and the endothelial marker CD31 were localized in the YS at E9.5 in all embryos investigated (14/14; Figure 3M; Figure S3F), whereas in the PAS region *Rag1*GFP$^+$ cells were rarely observed (Figure 3N). Notably, the majority of *Rag1*GFP$^+$ cells in the YS were predominantly located in close proximity to the primitive vascular plexus, rather than in large vessels (Figures 3M–3N; Figure S3F). In line with these data, we also observed transcriptional expression of *Rag2* and *Il7r* in E9.5 YS but little or no expression in E8.5 embryos or E9.5 PAS (Figure 3O). These data are most compatible with Lin$^-$Kit$^+$*Rag1*GFP$^+$IL7R$\alpha^+$ cells originating in E9.5 YS. However, because the connection between the YS and intraembryonic blood vessels occurs already at E8.5, we next dissected the YS and PAS regions from *Rag1*GFP$^+$ embryos before circulation was established ($\leq$6 somite pairs [sp]), short-term cultured the whole explants, and performed whole-mount immunolabeling (Cumano et al., 1996). Strikingly, in six out of ten YS explants, *Rag1*GFP$^+$ cells coexpressing CD45 and CD31 emerged after 48 hr, as did expression of *Il7r* and *sIgh* (Figures 3P and 3Q), whereas at the same time no *Rag1*GFP$^+$ cells were generated by the precirculation PAS explants (seven embryos) (Figure S3G), supporting that *Rag1*GFP$^+$IL7R$\alpha^+$ lymphomyeloid-restricted progenitors arise de novo in the YS at E9.5.

## *Rag1*$^+$ Immune-Restricted Progenitors Contribute to Fetal Lymphopoiesis and Myelopoiesis In Vivo

It is important to establish to what degree early lymphoid progenitors with sustained myeloid lineage potential in vitro contribute toward generation of myeloid cells under in vivo physiologically relevant conditions. Recent studies exploring this in adult hematopoiesis have questioned the physiological relevance of the residual myeloid potential of early lymphomyeloid progenitors (Boyer et al., 2011; Schlenner et al., 2010; Welner et al., 2009). Thus, although our in vitro experiments demonstrated that embryonic immune-restricted progenitors sustain lymphoid and GM but little or no MkE lineage potentials, they could not establish the contribution of these *Rag1*-expressing progenitors to different hematopoietic cell lineages during embryonic development. Thus, we applied a *Rag1-Cre* fate mapping in which only cells expressing *Rag1* or their progeny will express a yellow fluorescent protein (YFP). As expected, virtually all B and T cells emerging later in the fetus were positive for YFP in E14.5 FL (Figures 4A–4B) as in adult BM (Figure S4A). Moreover, *Rag1* expressing progenitors did not contribute to the Mk or E lineages, as predicted by our negative in vitro findings and the lack of MkE transcriptional priming (Figure 4A; Figures S4A and S4B). However, in contrast to the adult BM, in which we could confirm that *Rag1* expressing progenitors contribute minimally, if at all, to the GM lineage (Figure S4A), 36% of cells of the GM lineage were YFP$^+$ in E11.5 and 16% in E14.5 FLs (Figures 4A, 4C, and 4D; Figures S4C–S4E). Moreover, while erythroid colony forming cells were YFP$^-$, 20% of granulocyte- and macrophage-containing colonies were YFP$^+$ in E14.5 FLs (Figures 4E and 4F). These fate-mapping studies not only confirm the immune-restricted potentials of Lin$^-$Kit$^+$*Rag1*GFP$^+$IL7R$\alpha^+$ progenitors under physiological conditions in the early embryo but they also demonstrate that early embryonic *Rag1*-expressing progenitors contribute extensively to generation of GM and lymphoid cells in the embryo. Interestingly, resident tissue macrophages in the form of microglia, liver Kupffer cells, and epidermal Langerhans cells that develop around E8.5 independently of definitive HSCs (Schulz et al., 2012) were only minimally labeled by YFP (Figure S4F), suggesting that these tissues macrophages emerge independently of Lin$^-$Kit$^+$*Rag1*GFP$^+$IL7R$\alpha^+$ lymphomyeloid progenitors, in agreement with an origin prior to the emergence of the herein identified lymphomyeloid-restricted progenitor.

## Upregulation of Lymphoid and Downregulation of MkE Lineage Programs in Immune-Restricted Progenitors Prior to Emergence of Definitive HSCs

Genetic experiments have suggested that adult and fetal hematopoiesis is largely regulated through distinct molecular pathways (Yuan et al., 2012). However, whereas the global gene expression profiles of adult HSCs and progenitors have been explored extensively, this has not been feasible with early embryonic progenitors, partly because they have largely yet to be prospectively identified but also because of the scarcity of distinct progenitor cells at these early stages of development. We applied a recently established protocol for global RNA sequencing of small cell numbers (Ramsköld et al., 2012) on purified immune-restricted progenitors in E9.5 YS and E10.5 and E11.5 FLs. We compared expression levels of published

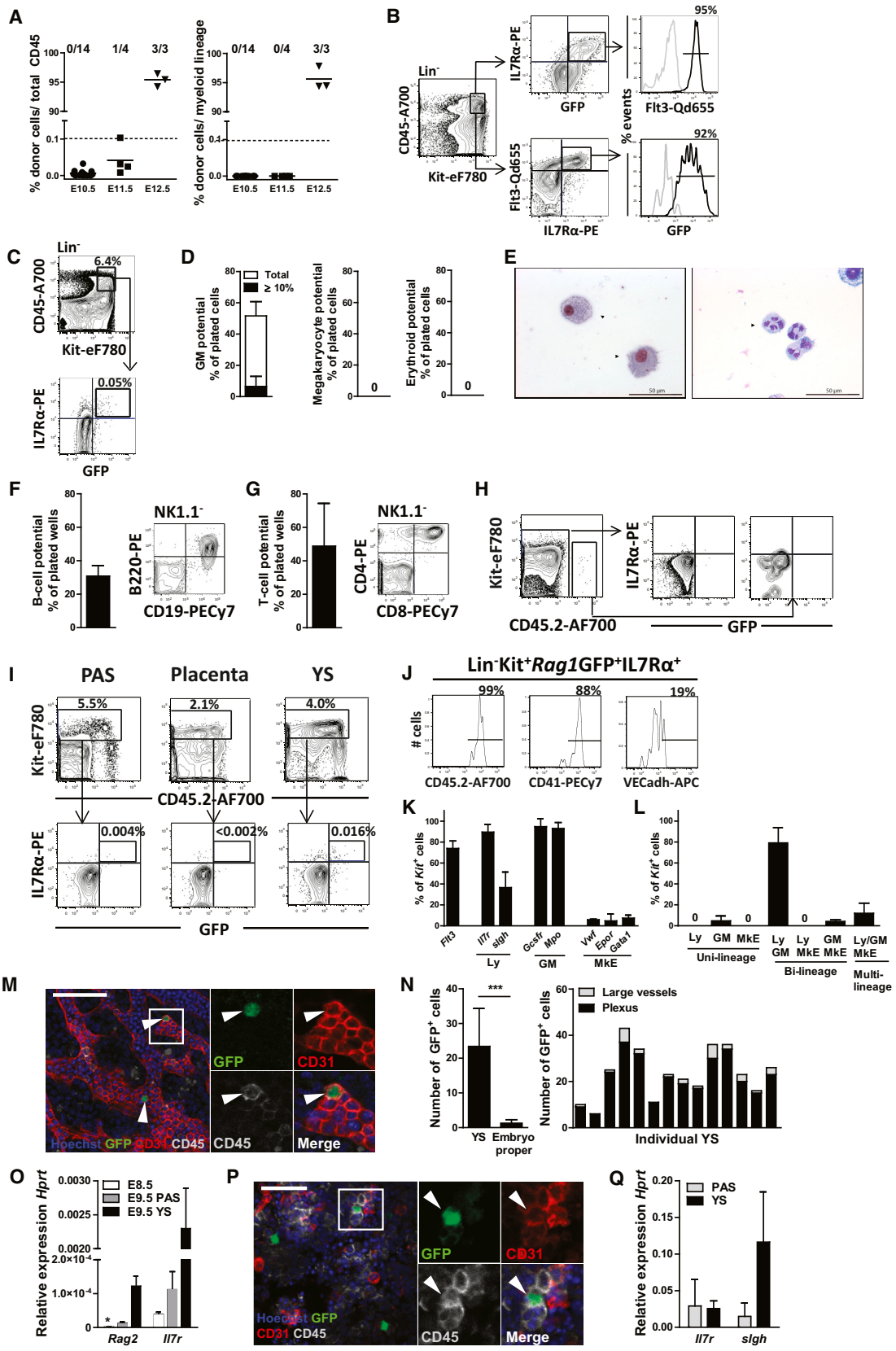


(legend on next page)

lineage-associated genes (Luc et al., 2012) in immune-restricted progenitors (Lin$^-$Kit$^+$*Rag1*GFP$^+$IL7R$\alpha^+$ or Lin$^-$Kit$^+$Flt3$^+$IL7R$\alpha^+$) with the corresponding Lin$^-$Kit$^+$ progenitors lacking expression of *Rag1*GFP, Flt3, and IL7R$\alpha$. This analysis demonstrated a striking upregulation of lymphoid and downregulation of MkE transcripts in E11.5 FL immune-restricted progenitors (Figure 5A), already evident in E10.5 FL and E9.5 YS progenitors (Figure S5A). In agreement with their virtual lack of MkE potential, key MkE regulatory transcripts were markedly downregulated (Figures 5A and 5B), whereas expression of multiple myeloid transcripts was sustained (Figures 5A and 5C). Early lymphoid transcripts were as expected almost undetectable in Lin$^-$Kit$^+$ *Rag1*GFP$^-$IL7R$\alpha^-$ and Lin$^-$Kit$^+$Flt3$^-$IL7R$\alpha^-$ progenitors, but markedly upregulated in immune-restricted progenitors at E9.5–E11.5 (Figures 5A and 5D; Figures S5A and S5B). In agreement with our single-cell PCR analysis, early B cell (*Cd79a*, *Ebf1*, *Pax5*, *Vpreb1)* and T cell (*Cd3e*, *Cd8a*, *Ptcra)* restricted transcripts were not expressed in E9.5 YS or E11.5 FL in neither the immune-restricted nor the control progenitors (Figures S5C and S5D), in support of B and T cell-restricted progenitors emerging later in fetal development, or at least not as part of the herein identified Lin$^-$Kit$^+$Rag1GFP$^+$IL7R$\alpha^+$ or Lin$^-$Kit$^+$Flt3$^+$ IL7R$\alpha^+$ immune-restricted progenitors.

Because the thymic anlage is seeded at E11.5 (Owen and Ritter, 1969), we also investigated the expression of genes implicated in regulation of thymus seeding progenitors (TSPs). Whereas Lin$^-$Kit$^+$*Rag1*GFP$^-$IL7R$\alpha^-$ and Lin$^-$Kit$^+$Flt3$^-$IL7R$\alpha^-$ cells expressed little or no *Ccr7* and *Ccr9*, encoding two chemokine receptors critically involved in the migration of embryonic TSPs to the thymus (Liu et al., 2006), both were markedly upregulated in E11.5 FL immune-restricted progenitors and in the case of *Ccr7* already at E9.5 (Figure 5E). Likewise, key regulatory genes in early T cell development such as *Gata3*, *Hes1*, *Notch1*, and *Tcf7* (Rothenberg, 2007) were markedly upregulated in E9.5 and E11.5 immune-restricted progenitors (Figure 5E), compatible with these progenitors possessing TSP potential.

When E9.5–E11.5 immune-restricted progenitors were compared to adult CLPs and LMPPs, investigated lymphoid genes were typically expressed at higher levels than in adult LMPPs (not further separated based on *Rag1*-GFP expression), but in most cases lower than adult CLPs (Figures 5D and 5E; Figure S5B). Selected MkE, GM, lymphoid, and TSP-related transcripts found to be differentially expressed in embryonic immune-restricted cells were further validated with quantitative PCR, confirming the same pattern of gene expression (Figures S6A–S6D). When analyzing the most significantly upregulated transcripts in E9.5 YS Lin$^-$Kit$^+$*Rag1*GFP$^+$IL7R$\alpha^+$ (compared to Lin$^-$Kit$^+$*Rag1*GFP$^-$IL7R$\alpha^-$) cells and in Lin$^-$Kit$^+$Flt3$^+$IL7R$\alpha^+$ E11.5 FL (compared to Lin$^-$Kit$^+$Flt3$^-$IL7R$\alpha^-$) cells, 67 transcripts were found to be commonly upregulated at both E9.5 and E11.5 (Figure 6; Tables S1–S3). Notably, the majority of these genes were almost exclusively overrepresented in Gene Ontology Categories related to development or function of the immune system (Figure 6), further supporting the emergence of lymphomyeloid-primed progenitors as an early embryonic commitment step toward establishing a fully competent mammalian immune system.

**Figure 3. Emergence of Lymphomyeloid Progenitors Coexpressing *Rag1*-GFP and IL7R$\alpha$ in E9.5 Embryos**

(A) Unfractionated E10.5 (1 FL/recipient), E11.5, and E12.5 (3–4 FLs per recipient) FL cells were competitively transplanted into lethally irradiated wild-type recipients. Left panel, total donor; right panel, myeloid reconstitution (dotted line represents detection level [background staining]; 0.1% donor contribution). Numbers indicate frequencies of mice reconstituted.

(B) Lin$^-$Kit$^+$*Rag1*GFP$^+$IL7R$\alpha^+$ cells in E11.5 FL were analyzed for expression of Flt3 (upper panel) and Lin$^-$Kit$^+$Flt3$^+$IL7R$\alpha^+$ cells for *Rag1*-GFP expression (lower panel). Mean percentages expression, gray line represents control (representative of 12 embryos investigated).

(C) Coexpression of IL7R$\alpha$ and *Rag1*-GFP in Lin$^-$Kit$^+$ progenitors in E10.5 (30–38 sp) FL cells. Mean percentage of total cells (5 experiments).

(D) Myeloid (single cells; left panel), megakaryocyte (single cells; middle panel), and erythroid (BFU-E; right panel) potential of Lin$^-$Kit$^+$*Rag1*GFP$^+$IL7R$\alpha^+$ E10.5 FL cells. Mean ± SD (>150 cells per assay, 3–5 experiments).

(E) Representative morphology of macrophages (left panel) and granulocytes (right panel) derived from sorted Lin$^-$Kit$^+$*Rag1*GFP$^+$IL7R$\alpha^+$ E10.5 FL cells as indicated by arrows.

(F) B cell (NK1.1$^-$CD19$^+$) and (G) T cell (NK1.1$^-$CD25$^+$Thy1.2$^{hi}$ and/or NK1.1$^-$CD4$^+$CD8$^+$) potential (4 cells per well, 3 experiments) of Lin$^-$Kit$^+$*Rag1*GFP$^+$IL7R$\alpha^+$ E10.5 FL cells. Mean percentages ± SD.

(H) Lack of expression of IL7R$\alpha$ and *Rag1*-GFP in the E8.5 (4–7 sp) conceptus. Viable cells were gated negative for mature lineage markers. Middle and right panels show expression analysis on CD45$^-$ and CD45$^+$ cells, respectively (2 experiments).

(I) Coexpression of IL7R$\alpha$ and *Rag1*-GFP in different tissues at E9.5 (14–26 sp); PAS (left panel), placenta (middle panel), and YS (right panel). Viable cells were gated negative for lineage markers; further gating is indicated with arrows. Mean percentages of total cells (3 experiments).

(J) Expression of CD45, CD41, and VE-Cadherin within the E9.5 YS Lin$^-$Kit$^+$*Rag1*GFP$^+$IL7R$\alpha^+$ population. Mean percentages of parent gate (3 experiments).

(K) Single-cell RT-PCR analysis in Lin$^-$Kit$^+$*Rag1*GFP$^+$IL7R$\alpha^+$ E9.5 YS progenitors and (L) combined transcriptional lineage priming patterns based on (K). Mean percentages ± SD of total *Kit*$^+$ cells (>91%; ≥50 cells, 2 experiments).

(M) Confocal image of a whole-mount immunolabeled E9.5 (23sp) *Rag1*GFP YS. Arrows indicate GFP$^+$ cells in the vascular plexus coexpressing CD31 and CD45. One of these (boxed area) is enlarged to show fluorescence in the individual channels. Original magnification 250×. Scale bar represents 100 μm.

(N) Left panel shows the number of GFP$^+$ cells per E9.5 YS and embryo proper respectively (mean ± SD, 11–14 embryos). ***p ≤ 0.001. Right panel shows distribution of GFP$^+$ cells within individual YS analyzed, as cells localized in the vascular plexus or in less branched larger vessels.

(O) Whole embryos at E8.5 and PAS and YS from E9.5 embryos were analyzed for *Rag2* and *Il7r* expression by quantitative PCR. Mean expression ± SD (normalized to *Hprt*; 2–4 biological replicates). *, not detected.

(P) Explant culture of precirculation *Rag1*-GFP YS (≤6 sp), were immunolabeled to detect the presence of *Rag1*GFP$^+$ cells. Representative confocal image of a YS explant (1 sp). The boxed area is enlarged and individual channels are shown for a GFP$^+$ cell coexpressing CD31 and CD45. Original magnification 250×. Scale bar represents 50 μm.

(Q) Precirculation PAS and YS were analyzed after 48 hr explant culture for *Il7r* and *sIgh* expression by quantitative PCR. Mean expression ± SD (normalized to *Hprt*; 3 biological replicates).

See also Figure S3.

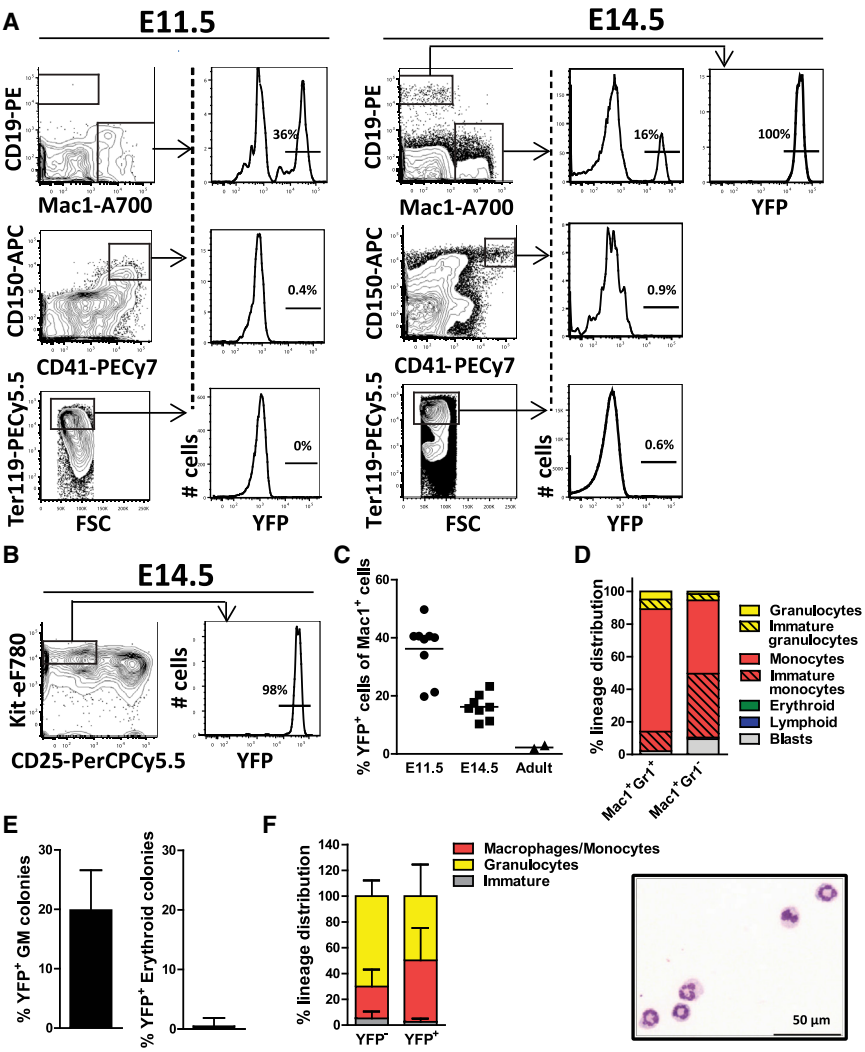


**Figure 4. *Rag1* Expressing Immune-Restricted Progenitors Contribute to Embryonic Myelopoiesis**

(A) *Rag1-Cre* fate mapping in E11.5 FL and E14.5 FL from *Rag1-Cre*$^{tg/+}$*R26R*$^{eYFP/+}$ embryos. Histograms show percentage of YFP$^+$ cells of total Mac1$^+$ (Ter119$^-$CD150$^-$CD41$^-$) myeloid cells, CD19$^+$ B cells, CD41$^+$CD150$^+$ (Ter119$^-$CD19$^-$Mac1$^-$Gr1$^-$) megakaryocytes, and Ter119$^+$ (CD19$^-$Mac1$^-$Gr1$^-$CD41$^-$CD150$^-$) erythroid cells. Mean percentages of parent gate (8 or 9 embryos).

(B) *Rag1-Cre* fate mapping in E14.5 thymus. Histogram shows percentage of YFP$^+$ cells of Kit$^+$CD25$^+$ (Lin$^-$CD4$^-$CD8$^-$) DN1 thymocytes. Mean percentages of parent gate (4 embryos).

(C) Percentages YFP$^+$ cells of total Mac1$^+$ myeloid cells in E11.5 FL, E14.5 FL, and adult BM. Each dot represents one individual mouse or embryo.

(D) Morphological distribution of cell types within Mac1$^+$Gr1$^+$YFP$^+$ (CD19$^-$B220$^-$Ter119$^-$CD150$^-$CD41$^-$) and Mac1$^+$Gr1$^-$YFP$^+$ (CD19$^-$B220$^-$Ter119$^-$CD150$^-$CD41$^-$) cells sorted from *Rag1-Cre*$^{tg/+}$*R26R*$^{eYFP/+}$ E14.5 FLs. Mean percentages (2 experiments).

(E) Mean percentages ± SD of YFP$^+$ GM (left) and erythroid (right) colonies generated from unfractionated E14.5 *Rag1-Cre*$^{tg/+}$*R26R*$^{eYFP/+}$ FL cells (GM; 12 individual embryos, >1000 colonies, Erythroid; 9 individual embryos, 218 colonies).

(F) Morphological distribution of cell types within YFP$^-$ and YFP$^+$ myeloid colonies generated from E14.5 *Rag1-Cre*$^{tg/+}$*R26R*$^{eYFP/+}$ FL cells in semi-solid culture. Mean percentage ± SD (5 embryos). Right panel shows representative granulocytes from YFP$^+$ colony.

See also Figure S4.

## DISCUSSION

Although other recent studies have carefully documented the emergence of progenitors with substantial lymphoid potential already in the E9.5 YS, as evaluated in cultures and upon transplantation (Yoshimoto et al., 2012), it has remained unclear whether or not this lymphoid potential comes from a multipotent progenitor in the YS or an already partially or fully lymphoid-restricted progenitor. *Ncx1* knockout embryos fail to develop a beating heart and therefore lack a circulation. Investigation of *Ncx1* null embryos provided compelling evidence for the emergence in the YS of progenitors with considerable lymphoid potential as established through their ability in long-term cultures and upon transplantation to produce fetal, as well as adult type, T cells (Yoshimoto et al., 2012). However, the progenitors responsible for this activity were not prospectively identified, and it was not established whether the cells producing only T cells in the long-term assays might also possess other lineage potentials. In fact, in another study it was shown that the same E9.5 YS cells also have B cell potential when assessed in other assays (Yoshimoto et al., 2011). The present studies suggest that the T and B lymphoid potential observed in the E9.5 YS by Yoshimoto et al. might derive at least in part from multipotent but lympho-myeloid-restricted progenitors.

Through prospective purification, molecular characterization, and fate mapping, the findings herein establish that extensive lymphoid transcriptional priming and lymphomyeloid-lineage restriction initiates in the YS at E9.5, earlier than previously recognized, before the emergence of definitive HSCs and establishment of FL hematopoiesis. This restriction occurs through the establishment of distinct immune-restricted progenitors with combined lymphoid and myeloid lineage potentials (Figure 7), defined by upregulation of specific regulators of lymphopoiesis: *Rag1*, Flt3, and IL7Rα, as well as a number of other lymphoid-specific transcripts. Importantly, single-cell lineage-potential assays, as well as in vivo fate mapping of their progeny during normal embryonic development, confirmed not only the virtual absence of MkE potentials but also the physiological and robust contribution to the myeloid (GM), as well as lymphoid, lineages in the developing embryo.

The lymphomyeloid-primed progenitors already detected in E9.5 YS and E10.5 FL represent the earliest identified embryonic progenitors in which specific and key lymphoid gene expression is initiated, coexpressed with myeloid genes, and paralleled by a distinct downregulation of MkE genes, similar to the LMPPs

identified later in development (Adolfsson et al., 2005; Månsson et al., 2007). The lymphoid genes expressed in these embryonic progenitors were early common lymphoid genes, whereas early B and T cell progenitor-specific genes were found to be negative, in agreement with previous studies supporting that B and T cell lineage commitment occurs later in FL hematopoiesis (Douagi et al., 2002), or at least not within the herein identified lymphomyeloid-restricted progenitors. Moreover, every $Lin^{-}Kit^{+}Flt3^{+}IL7R\alpha^{+}$ progenitor cell expressing these lymphoid genes coexpressed at the single-cell level myeloid lineage genes even in the E11.5 FL, whereas none of them expressed signature genes of the earliest B (*Pax5*) and T (*Ptcra*) cell-restricted progenitors. In light of these findings, we suggest that earlier studies implicating the emergence of fully B or T lymphoid-restricted progenitors already in the E10–10.5 AGM region and fetal circulation, based on evaluation of clonal lineage output of heterogenous progenitor populations (Ikawa et al., 2004; Ohmura et al., 1999), might have missed the myeloid output of lymphomyeloid-restricted progenitors as a result of the short lifespan of myeloid cells in culture. Regardless, establishment of whether also fully lymphoid-restricted progenitors might emerge prior to definitive HSCs would require their prospective purification and molecular evidence of fully lymphoid-restricted progenitor cells.

The most significantly upregulated genes in embryonic lymphomyeloid-restricted progenitors were almost exclusively related to development or function of the immune system, including genes demonstrated to be of critical importance for establishment of thymopoiesis (Rothenberg, 2007), implicating early embryonic lymphomyeloid progenitors as candidate TSPs. Findings of Yoshimoto et al. (2012) showing that there are cells with thymus reconstitution potential already in the E9.5 YS and PAS region, combined with our identification in E9.5 YS of distinct lymphomyeloid-primed progenitors with upregulated expression of genes for chemokine receptors, critically involved in migration of TSPs to the embryonic thymus, raises the possibility that TSPs responsible for initiation of thymopoiesis in the embryo might be generated in the YS.

Our analysis of different hematopoietic regions in the embryo by FACS, whole-mount imaging, and PCR analysis suggest that the identified lymphomyeloid-restricted progenitors emerge first in the YS at E9.5, a finding further supported by precirculation explant short-term cultures of the YS and PAS regions. The identity of the hematopoietic stem-progenitor cells giving rise to this first wave of lymphomyeloid-restricted progenitors remains to be established. Although their early emergence rules out an origin from definitive HSCs, they might derive from hemogenic endothelium in E9.5 YS as suggested in recent studies (Yoshimoto et al., 2012) and as further supported by our finding of *Rag1*$GFP^{+}$ cells in the primitive vascular plexus in the E9.5 YS. Alternatively, they might derive from multipotent progenitors in the YS, also possessing MkE potential, or potentially from recently identified candidate pre-HSCs (Figure 7B).

Previous studies have proposed the existence of mouse lymphomyeloid-restricted progenitors in FL hematopoiesis (Cumano et al., 1992; Katsura and Kawamoto, 2001; Lacaud et al., 1998), and the LMPP was later prospectively identified in adult hematopoiesis as well as in E14.5 FL (Adolfsson et al., 2005; Arinobu et al., 2007; Månsson et al., 2007). Although collectively these studies provided compelling experimental support for a revised hematopoietic hierarchy with separate CMP and lymphomyeloid immune-restricted pathways (reviewed in (Luc et al., 2008b), this has not precluded the conceptually classical CMP-CLP roadmap from still prevailing in the literature (Orkin and Zon, 2008a, b; Seita and Weissman, 2010). This controversy reflects in part that all studies supporting either model have relied exclusively on the ability of nonphysiological in vitro and in vivo reconstitution assays to uncover lineage potentials of the prospectively purified progenitor cells. Thus, although these studies have been instrumental for our current understanding of lineage commitment, the assays applied do have intrinsic caveats (Richie Ehrlich et al., 2011). Perhaps even more relevant, uncovering of multiple lineage potentials of a progenitor cell in vitro or upon in vivo transplantation into conditioned recipients does not address whether and to what degree the progenitor in question contributes (or not) under normal in vivo physiological conditions toward the different cell lineage potentials.

Although genetic fate-mapping experiments in vivo could address these fundamentally important questions, it remains a considerable challenge to develop strategies that would faithfully allow lineage tracing of distinct progenitor cells. Results from recent *Flt3* lineage-tracing studies questioned the physiological relevance of an early lymphomyeloid lineage-restriction step in hematopoiesis (Boyer et al., 2011, 2012), although the conclusions were limited by *Flt3* expression initiating already in fully multipotent progenitors (Boyer et al., 2012; Buza-Vidas et al., 2011). Another recent *Il7r* fate-mapping study also questioned the myeloid contribution and the physiological significance of a lymphomyeloid-restricted pathway (Schlenner et al., 2010; Schlenner and Rodewald, 2010), as did *Rag1* fate mapping in adult hematopoiesis (Welner et al., 2009). However, only a small fraction of adult lymphomyeloid-restricted LMPPs express *Il7r* or *Rag1* (Adolfsson et al., 2005; Luc et al., 2008a), and $Rag1^{+}$ LMPPs have considerably reduced myeloid potential as compared to $Rag1^{-}$ LMPPs (Luc et al., 2008a). In contrast, we here demonstrate that early embryonic lymphomyeloid-restricted progenitors express much higher levels of *Il7r* and *Rag1*, and when applying *Rag1-Cre* fate mapping, we could for the first time demonstrate that lymphomyeloid-restricted progenitors contribute extensively to myelopoiesis, as well as lymphopoiesis during normal fetal development. Of equal importance, we found no significant contribution of *Rag1*-expressing progenitors to the MkE lineages in vivo, confirming their immune-restricted role. Thus, our combined lineage potential and fate-mapping studies establish the existence of lymphomyeloid-restricted progenitors in early embryonic hematopoiesis prior to emergence of definitive HSCs, and their physiological contribution to both the myeloid innate and lymphoid adaptive immune system. Notably, the existence of lymphomyeloid-restricted progenitors has also recently been implicated in early postnatal and adult human hematopoiesis (Doulatov et al., 2010; Goardon et al., 2011; Kohn et al., 2012).

The identification of an embryonic immune-restricted progenitor is of relevance for childhood acute lymphoblastic leukemia (cALL), the most common form of pediatric cancer. Preleukemic translocations in cALL frequently occur in utero in unidentified

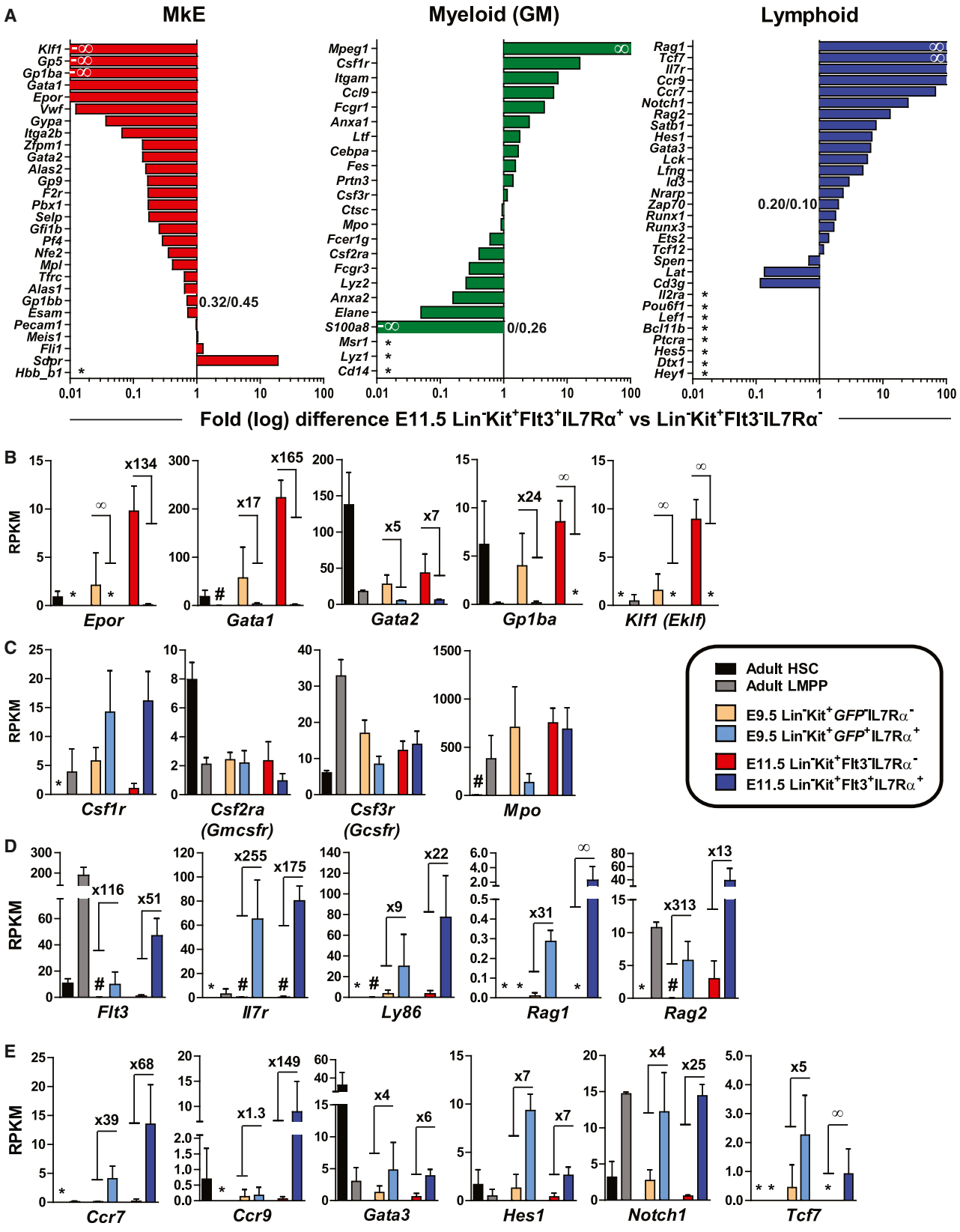


(legend on next page)

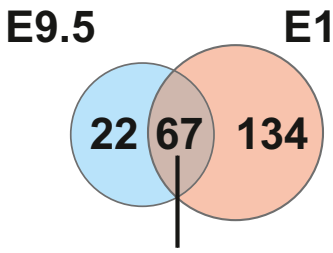


**Statistically over-represented Gene Ontology Categories**

| GO annotation | FDR | Coverage |
|---|---|---|
| B cell activation | 2.42E-02 | 6 / 147 |
| immunoglobulin production | 2.42E-02 | 5 / 69 |
| T cell differentiation | 2.42E-02 | 6 / 154 |
| external side of plasma membrane | 2.42E-02 | 7 / 229 |
| production of molecular mediator of immune response | 3.34E-02 | 5 / 97 |
| T cell activation | 3.93E-02 | 7 / 274 |
| B cell proliferation | 6.68E-02 | 4 / 60 |
| lymphocyte differentiation | 6.68E-02 | 6 / 203 |
| regulation of lymphocyte differentiation | 2.68E-01 | 4 / 88 |
| leukocyte differentiation | 3.80E-01 | 6 / 296 |

**Commonly upregulated genes in E9.5 and E11.5 immune-restricted progenitors**

| | | | | | | |
|---|---|---|---|---|---|---|
| *2010001M09Rik* | *Clec12a* | *Gem* | *Ift57* | *Mycn* | *Ptprc* | *Stc1* |
| *Abcg3* | *Ctnnd2* | *Gimap6* | *Il1r2* | *Napsa* | *Pygm* | *Tifa* |
| *Alcam* | *Cybb* | *Gimap7* | *Il7r* | *Notch1* | *Rag2* | *Tnip3* |
| *Bfsp2* | *Dpysl2* | *Gngt2* | *Klrd1* | *P2ry12* | *Rgs1* | *Tnni2* |
| *Calcrl* | *Dusp6* | *Gpr171* | *Lax1* | *P2ry14* | *Runx2* | *Tsc22d1* |
| *Ccnd2* | *Emcn* | *Gpr65* | *Lsp1* | *Plk2* | *Serpinb1a* | *Tshz3* |
| *Cd27* | *Entpd1* | *Gsn* | *Ly86* | *Ppp1r16b* | *Sesn1* | *Zcchc18* |
| *Cd33* | *Ets1* | *Hmgn3* | *Marcks* | *Prss2* | *Snn* | |
| *Cd7* | *Fgd2* | *Ifi203* | *Mn1* | *Psmb8* | *Sp100* | |
| *Cdh17* | *Flt3* | *Ifitm3* | *Mndal* | *Psmb9* | *St8sia4* | |

**Figure 6. Upregulation of Immune-Related Genes in E9.5 Yolk Sac and E11.5 Fetal Liver Immune-Restricted Progenitors**

Venn diagram showing overlap of upregulated genes in E9.5 YS Lin$^-$Kit$^+$ *Rag1*GFP$^+$IL7R$\alpha^+$ (compared to Lin$^-$Kit$^+$*Rag1*GFP$^-$IL7R$\alpha^-$) cells and E11.5 FL Lin$^-$Kit$^+$Flt3$^+$IL7R$\alpha^+$ (compared to Lin$^-$Kit$^+$Flt3$^-$IL7R$\alpha^-$) cells. Of these 67 overlapping genes, 64 were also upregulated in E10.5 FL Lin$^-$Kit$^+$ *Rag1*GFP$^+$IL7R$\alpha^+$ cells (data not shown). Also shown are Gene Ontology Categories in which common upregulated genes were significantly enriched. Note that almost all of these categories are related to the immune system.
See also Figures S5 and S6 and Tables S1–S3.

progenitors (Greaves and Wiemels, 2003), also resulting in poor-prognosis biphenotypic leukemias with characteristics of the lymphoid and the GM, but not MkE lineages (Béné, 2009). Our identification of immune-restricted progenitors emerging in the embryo prior to definitive HSCs and establishment of FL hematopoiesis will also facilitate a better understanding of the molecular determinants and cellular pathways required for the development of a fully competent innate and adaptive immune system and of how this process is dysregulated in the conglomerate of congenital immune deficiencies (Cunningham-Rundles and Ponda, 2005).

## EXPERIMENTAL PROCEDURES

### Animals and Cell Preparations

Embryos were obtained by timed mating, with the morning of vaginal plug detection set as E0.5. Animal experiments were performed according to regulations by the local animal ethics committee at Lund University and the UK Home Office at University of Oxford. For details, see Supplemental Experimental Procedures.

### Fluorescence Activated Cell Sorting

Dissected tissues and adult BM (>8 weeks old) were treated with purified anti-CD16/32 (Fc-block) and stained with antibodies specified in Supplemental Experimental Procedures. Adult HSCs and progenitors were defined with the following markers: adult HSCs; LSKCD150$^+$CD48$^-$, LMPPs; LSKFlt3$^{hi}$, CLPs; Lin$^-$CD11c$^-$Ly6C$^-$CD19$^-$B220$^-$Ly6D$^-$Kit$^{lo}$Sca$^{lo}$Flt3$^+$IL7R$\alpha^+$; proB cells; Kit$^+$CD19$^+$B220$^+$CD43$^+$.

### In Vitro Cultures

Evaluation of MkE and GM lineage potentials was performed as previously described with minor modifications (Supplemental Experimental Procedures) (Adolfsson et al., 2005; Luc et al., 2008a; Månsson et al., 2007). Erythroid lineage potential was additionally evaluated on Op9 coculture with cytokines as specified in Supplemental Experimental Procedures. Clones were considered positive for erythroid development if cells had a Ter119$^+$CD71$^+$ (Mac1$^-$Gr1$^-$CD150$^-$CD41$^-$) FACS profile and/or by positive morphology on May-Grünwald/Giemsa stained cytospins. For evaluation of lymphoid potential or combined potential, cells were plated onto Op9 or Op9DL1 stroma cells with cytokines as previously described (Månsson et al., 2007) (see Supplemental Experimental Procedures).

### *Rag1-Cre* Fate Mapping

*Rag1-Cre*$^{tg/+}$*R26R*$^{eYFP/+}$ and littermate *Rag1-Cre*$^{+/+}$*R26R*$^{eYFP/+}$ control adult BM and FLs (E11.5 and E14.5) were stained as specified in Supplemental Experimental Procedures. Adult *Flt3-Cre*$^{tg/+}$*R26R*$^{eYFP/+}$ BM was used as a positive control to demonstrate that the R26 promoter sustains YFP expression in all mature (B, T, Mk, and E) lineages as previously shown (Buza-Vidas et al., 2011) (for further details, see Supplemental Experimental Procedures).

### Explant Cultures and Imaging

The YS and PAS regions were dissected from staged embryos ($\leq$6 sp) prior to establishment of circulation as previously described (Cumano et al., 1996), cultured individually, and then whole-mount immunolabeled, or explants were taken for quantitative PCR (see Supplemental Experimental Procedures).

### In Vivo Reconstitution Experiments

FL cells from E10.5 (32–44 sp), E11.5, and E12.5 CD45.2 embryos were transplanted together with 250,000–300,000 competitor CD45.1 BM cells into lethally irradiated (2 × 450cGy) C57/Bl6 WT CD45.1 mice, either intravenously or intrafemorally as specified (in some cases CD45.1 embryos were used and transplanted into CD45.2 WT recipients). Peripheral blood (PB) analyses were conducted at 15–17 weeks (see Supplemental Experimental Procedures). Mice were considered reconstituted if $\geq$0.1% donor contribution to total CD45$^+$ cells was achieved.

**Figure 5. Upregulation of Lymphoid and Downregulation of MkE Transcriptional Programs in Early Embryonic Immune-Restricted Progenitors**

(A) E11.5 Lin$^-$Kit$^+$Flt3$^+$IL7R$\alpha^+$ and Lin$^-$Kit$^+$Flt3$^-$IL7R$\alpha^-$ E11.5 FL cells were subjected to global RNA sequencing and analyzed for differences in expression levels of previously published lineage-associated (MkE, Myeloid [GM], and Lymphoid) programs (Luc et al., 2012). Mean fold differences in RPKM ( = reads per kilobase of exon model per million mapped reads) values are shown on a $\log_{10}$ scale. *, RPKM $\leq$0.05 for both cell populations. For genes with expression $\leq$0.5 RPKM for both cell populations, specific values are indicated next to bars. $\infty$, infinity.
(B–E) Expression as determined by RNA sequencing of (B) MkE, (C) GM, (D) lymphoid, and (E) thymus-seeding progenitor related genes, in E9.5 YS and E11.5 FL progenitors. Adult HSCs and adult LMPPs are shown as controls. Graph legend for (B)–(E) is shown in the box to the right. Numbers indicate fold difference. Mean RPKM ± SD (2–3 experiments).
*, not detected; #, expressed but at too low level to be visualized on the applied scale; and $\infty$, infinity as not detected in one of the two cell populations in either experiment.
See also Figures S5 and S6.

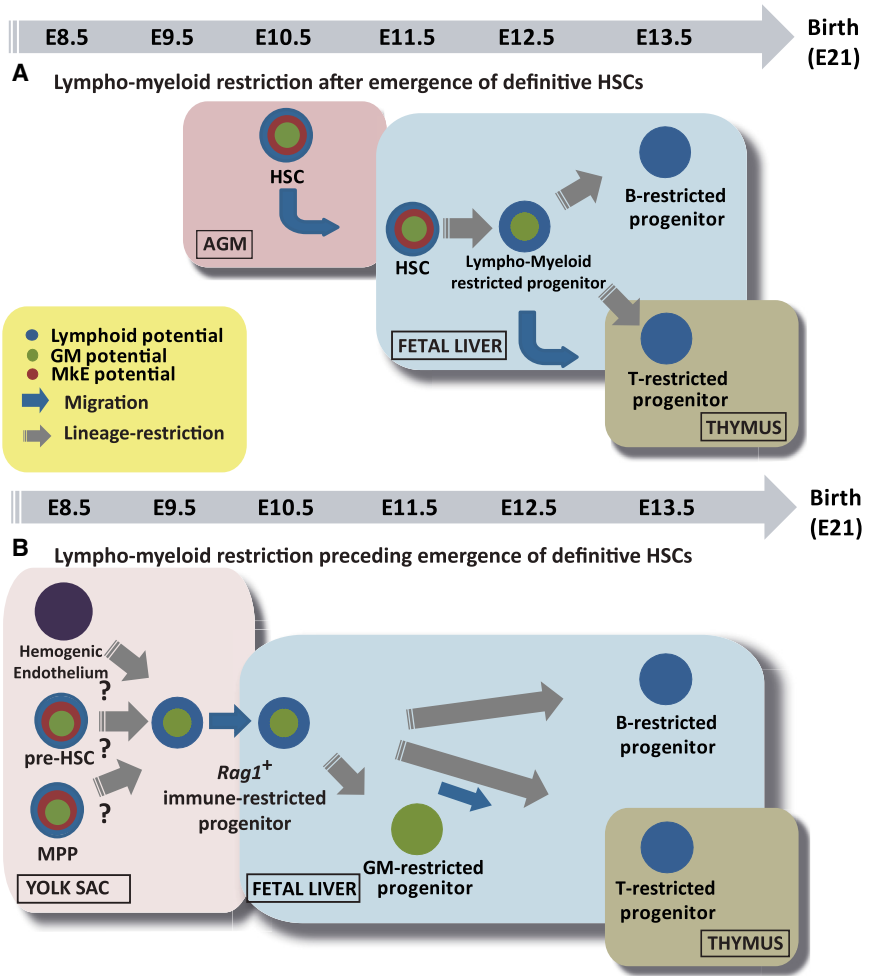


**Figure 7. Lymphoid-Myeloid Lineage Restriction in the Mouse Embryo Occurs Independently of and Precedes Emergence of Definitive HSCs**

(A) Lymphomyeloid lineage restriction after emergence of definitive HSCs. Model for initiation of lymphomyeloid lineage restriction based on published data suggesting that the first lymphoid restriction steps occurs after emergence of definitive HSCs in the aorta-gonad-mesonephros (AGM) region and their subsequent seeding of the fetal liver. According to this model, the first lympho-myeloid progenitors (for which the exact lineage potentials at the single-cell level remains unclear) emerge at about E12 followed by generation of B and T lymphoid restricted progenitors at E13.5 or later.

(B) Initiation of lymphomyeloid lineage restriction preceding emergence of definitive HSCs.

Initiation of lymphomyeloid lineage restriction based on the identification of a *Rag1*GFP$^{+}$IL7R$\alpha^{+}$ immune-restricted progenitor at E9.5 in yolk sac and E10.5 in fetal liver, prior to emergence of definitive HSCs in the AGM region. This early immune-restricted progenitor contributes to myelopoiesis (GM) already at E11.5 and later to B and T cell restricted progenitors but little or not to megakaryo-erythropoiesis. The immune-restricted progenitor emerges in the yolk sac prior to definitive HSCs, which is compatible with originating from proposed hemogenic endothelium, pre-HSCs, or earlier multipotent progenitors, as indicated.

### Single-Cell and Quantitative PCR

Multiplex single-cell RT-PCR and multiplex quantitative real-time PCR analysis (BioMark 48.48 or 96.96 Dynamic Array platform [Fluidigm] with TaqMan Gene Expression Assays [Applied Biosystems]) were performed as described in Supplemental Experimental Procedures (Adolfsson et al., 2005; Månsson et al., 2007).

### RNA Sequencing

Samples for RNA sequencing (73–100 cells) were prepared with the SMARTer Ultra Low RNA kit for Illumina Sequencing (Clontech) and sequenced and analyzed as previously described (Ramsköld et al., 2012) (see Supplemental Experimental Procedures).

### Statistics

Statistical significance was determined by one or two-tailed (depending on hypothesis) unpaired Mann Whitney (nonparametric) test. The significance level was set at $p \leq 0.05$. Unless otherwise stated, data are shown as mean ± SD.

## ACCESSION NUMBERS

The RNA sequencing data have been deposited in NCBI GEO under accession number GSE50896.

## SUPPLEMENTAL INFORMATION

Supplemental Information includes six figures, three tables, and Supplemental Experimental Procedures and can be found with this article online at http://dx.doi.org/10.1016/j.stem.2013.08.012.

## AUTHOR CONTRIBUTIONS

S.E.W.J. and C.B. conceptualized and designed the overall research, analyzed the data, and wrote the manuscript. C.B., M.L., S.L., A.H., J.C., and J.C.A.G. performed and analyzed experiments. M.L. did the micromanipulation of single cells. E.A., G.S., and M.B. performed the embryonic dissections; E.A. performed the whole mount imaging and M.B. contributed with expert advice and input on design and analysis of embryonic studies. I.G. performed and designed the explant culture experiments. P.S.W., I.C.M., Q.D., and R.S. performed and analyzed the RNA sequencing data. D.A. and A.J.M. performed and analyzed the quantitative PCR data, and A.J.M. analyzed morphology. T.B.-J. and L.M. contributed in vitro culture experiments. T.C.L. analyzed transplantation experiments, and S.K., A.P., and C.T.J. contributed and performed the initiating experiments of the study. E.G.P. and F.G. performed and analyzed the tissue macrophage experiments. E.S. contributed with advice on execution of experiments. All authors read and approved the final manuscript.

## ACKNOWLEDGMENTS

The authors thank Lilian Wittmann, Ingbritt Åstrand-Grundström, and Hanane Boukarabila for skillful technical assistance, the Biomedical Services at Oxford University for expert animal support, and Sally-Ann Clark, Paul Sopp, and the WIMM FACS facility for FACS support. Åsa Björklund, Daniel Ramsköld, and Ersen Kavak are thanked for skillful technical assistance with the RNA sequencing. This work was supported by a programme grant (H4RPLK0) from the Medical Research Council UK (S.E.W.J.), Knut och Alice

Wallenberg Foundation (WIRM; S.E.W.J.), StratRegen, KI (S.E.W.J.), EU-FP7 EuroSyStem Integrated projects (S.E.W.J.), ALF (Government Public Health Grant; C.B.), the Hemato-Linné grant (Swedish Research Council Linnaeus; S.E.W.J.), the MRC Molecular Haematology Unit core award (M.F.T.R.d.-B., E.A., S.E.W.J.), a Leukaemia and Lymphoma Research project grant (M.B., G.S.), Swedish Cancer foundation (A.H.), Swedish Society of Medicine (A.H.), Crafoord Foundation (A.H.), Georg Danielsson's foundation (A.H.), and the Leukaemia and Lymphoma Research Senior Bennett Fellowship (A.J.M.).

Received: February 16, 2013
Revised: July 21, 2013
Accepted: August 28, 2013
Published: September 19, 2013

## REFERENCES

Adolfsson, J., Månsson, R., Buza-Vidas, N., Hultquist, A., Liuba, K., Jensen, C.T., Bryder, D., Yang, L., Borge, O.J., Thoren, L.A., et al. (2005). Identification of Flt3+ lympho-myeloid stem cells lacking erythro-megakaryocytic potential a revised road map for adult blood lineage commitment. Cell *121*, 295–306.

Akashi, K., Traver, D., Miyamoto, T., and Weissman, I.L. (2000). A clonogenic common myeloid progenitor that gives rise to all myeloid lineages. Nature *404*, 193–197.

Arinobu, Y., Mizuno, S., Chong, Y., Shigematsu, H., Iino, T., Iwasaki, H., Graf, T., Mayfield, R., Chan, S., Kastner, P., and Akashi, K. (2007). Reciprocal activation of GATA-1 and PU.1 marks initial specification of hematopoietic stem cells into myeloerythroid and myelolymphoid lineages. Cell Stem Cell *1*, 416–427.

Béné, M.C. (2009). Biphenotypic, bilineal, ambiguous or mixed lineage: strange leukemias! Haematologica *94*, 891–893.

Boyer, S.W., Schroeder, A.V., Smith-Berdan, S., and Forsberg, E.C. (2011). All hematopoietic cells develop from hematopoietic stem cells through Flk2/Flt3-positive progenitor cells. Cell Stem Cell *9*, 64–73.

Boyer, S.W., Beaudin, A.E., and Forsberg, E.C. (2012). Mapping differentiation pathways from hematopoietic stem cells using Flk2/Flt3 lineage tracing. Cell Cycle *11*, 3180–3188.

Buza-Vidas, N., Woll, P., Hultquist, A., Duarte, S., Lutteropp, M., Bouriez-Jones, T., Ferry, H., Luc, S., and Jacobsen, S.E. (2011). FLT3 expression initiates in fully multipotent mouse hematopoietic progenitor cells. Blood *118*, 1544–1548.

Cumano, A., Paige, C.J., Iscove, N.N., and Brady, G. (1992). Bipotential precursors of B cells and macrophages in murine fetal liver. Nature *356*, 612–615.

Cumano, A., Dieterlen-Lievre, F., and Godin, I. (1996). Lymphoid potential, probed before circulation in mouse, is restricted to caudal intraembryonic splanchnopleura. Cell *86*, 907–916.

Cunningham-Rundles, C., and Ponda, P.P. (2005). Molecular defects in T- and B-cell primary immunodeficiency diseases. Nat. Rev. Immunol. *5*, 880–892.

Douagi, I., Vieira, P., and Cumano, A. (2002). Lymphocyte commitment during embryonic development, in the mouse. Semin. Immunol. *14*, 361–369.

Doulatov, S., Notta, F., Eppert, K., Nguyen, L.T., Ohashi, P.S., and Dick, J.E. (2010). Revised map of the human progenitor hierarchy shows the origin of macrophages and dendritic cells in early lymphoid development. Nat. Immunol. *11*, 585–593.

Forsberg, E.C., Serwold, T., Kogan, S., Weissman, I.L., and Passegué, E. (2006). New evidence supporting megakaryocyte-erythrocyte potential of flk2/flt3+ multipotent hematopoietic progenitors. Cell *126*, 415–426.

Goardon, N., Marchi, E., Atzberger, A., Quek, L., Schuh, A., Soneji, S., Woll, P., Mead, A., Alford, K.A., Rout, R., et al. (2011). Coexistence of LMPP-like and GMP-like leukemia stem cells in acute myeloid leukemia. Cancer Cell *19*, 138–152.

Greaves, M.F., and Wiemels, J. (2003). Origins of chromosome translocations in childhood leukaemia. Nat. Rev. Cancer *3*, 639–649.

Hu, M., Krause, D., Greaves, M., Sharkis, S., Dexter, M., Heyworth, C., and Enver, T. (1997). Multilineage gene expression precedes commitment in the hemopoietic system. Genes Dev. *11*, 774–785.

Ikawa, T., Masuda, K., Lu, M., Minato, N., Katsura, Y., and Kawamoto, H. (2004). Identification of the earliest prethymic T-cell progenitors in murine fetal blood. Blood *103*, 530–537.

Katsura, Y., and Kawamoto, H. (2001). Stepwise lineage restriction of progenitors in lympho-myelopoiesis. Int. Rev. Immunol. *20*, 1–20.

Kawamoto, H., Ikawa, T., Ohmura, K., Fujimoto, S., and Katsura, Y. (2000). T cell progenitors emerge earlier than B cell progenitors in the murine fetal liver. Immunity *12*, 441–450.

Kieusseian, A., Brunet de la Grange, P., Burlen-Defranoux, O., Godin, I., and Cumano, A. (2012). Immature hematopoietic stem cells undergo maturation in the fetal liver. Development *139*, 3521–3530.

Kohn, L.A., Hao, Q.L., Sasidharan, R., Parekh, C., Ge, S., Zhu, Y., Mikkola, H.K., and Crooks, G.M. (2012). Lymphoid priming in human bone marrow begins before expression of CD10 with upregulation of L-selectin. Nat. Immunol. *13*, 963–971.

Kondo, M., Weissman, I.L., and Akashi, K. (1997). Identification of clonogenic common lymphoid progenitors in mouse bone marrow. Cell *91*, 661–672.

Kumaravelu, P., Hook, L., Morrison, A.M., Ure, J., Zhao, S., Zuyev, S., Ansell, J., and Medvinsky, A. (2002). Quantitative developmental anatomy of definitive haematopoietic stem cells/long-term repopulating units (HSC/RUs): role of the aorta-gonad-mesonephros (AGM) region and the yolk sac in colonisation of the mouse embryonic liver. Development *129*, 4891–4899.

Lacaud, G., Carlsson, L., and Keller, G. (1998). Identification of a fetal hematopoietic precursor with B cell, T cell, and macrophage potential. Immunity *9*, 827–838.

Liu, C., Saito, F., Liu, Z., Lei, Y., Uehara, S., Love, P., Lipp, M., Kondo, S., Manley, N., and Takahama, Y. (2006). Coordination between CCR7- and CCR9-mediated chemokine signals in prevascular fetal thymus colonization. Blood *108*, 2531–2539.

Luc, S., Anderson, K., Kharazi, S., Buza-Vidas, N., Böiers, C., Jensen, C.T., Ma, Z., Wittmann, L., and Jacobsen, S.E. (2008a). Down-regulation of Mpl marks the transition to lymphoid-primed multipotent progenitors with gradual loss of granulocyte-monocyte potential. Blood *111*, 3424–3434.

Luc, S., Buza-Vidas, N., and Jacobsen, S.E. (2008b). Delineating the cellular pathways of hematopoietic lineage commitment. Semin. Immunol. *20*, 213–220.

Luc, S., Luis, T.C., Boukarabila, H., Macaulay, I.C., Buza-Vidas, N., Bouriez-Jones, T., Lutteropp, M., Woll, P.S., Loughran, S.J., Mead, A.J., et al. (2012). The earliest thymic T cell progenitors sustain B cell and myeloid lineage potential. Nat. Immunol. *13*, 412–419.

Månsson, R., Hultquist, A., Luc, S., Yang, L., Anderson, K., Kharazi, S., Al-Hashmi, S., Liuba, K., Thorén, L., Adolfsson, J., et al. (2007). Molecular evidence for hierarchical transcriptional lineage priming in fetal and adult stem cells and multipotent progenitors. Immunity *26*, 407–419.

Masuda, K., Kubagawa, H., Ikawa, T., Chen, C.C., Kakugawa, K., Hattori, M., Kageyama, R., Cooper, M.D., Minato, N., Katsura, Y., and Kawamoto, H. (2005). Prethymic T-cell development defined by the expression of paired immunoglobulin-like receptors. EMBO J. *24*, 4052–4060.

Medvinsky, A., and Dzierzak, E. (1996). Definitive hematopoiesis is autonomously initiated by the AGM region. Cell *86*, 897–906.

Medvinsky, A., Rybtsov, S., and Taoudi, S. (2011). Embryonic origin of the adult hematopoietic system: advances and questions. Development *138*, 1017–1031.

Ohmura, K., Kawamoto, H., Fujimoto, S., Ozaki, S., Nakao, K., and Katsura, Y. (1999). Emergence of T, B, and myeloid lineage-committed as well as multipotent hemopoietic progenitors in the aorta-gonad-mesonephros region of day 10 fetuses of the mouse. J. Immunol. *163*, 4788–4795.

Orkin, S.H., and Zon, L.I. (2008a). Hematopoiesis: an evolving paradigm for stem cell biology. Cell *132*, 631–644.

Orkin, S.H., and Zon, L.I. (2008b). SnapShot: hematopoiesis. Cell *132*, 712.

Osawa, M., Hanada, K.-I., Hamada, H., and Nakauchi, H. (1996). Long-term lymphohematopoietic reconstitution by a single CD34-low/negative hematopoietic stem cell. Science *273*, 242–245.

Owen, J.J., and Ritter, M.A. (1969). Tissue interaction in the development of thymus lymphocytes. J. Exp. Med. *129*, 431–442.

Ramsköld, D., Luo, S., Wang, Y.C., Li, R., Deng, Q., Faridani, O.R., Daniels, G.A., Khrebtukova, I., Loring, J.F., Laurent, L.C., et al. (2012). Full-length mRNA-Seq from single-cell levels of RNA and individual circulating tumor cells. Nat. Biotechnol. *30*, 777–782.

Richie Ehrlich, L.I., Serwold, T., and Weissman, I.L. (2011). In vitro assays misrepresent in vivo lineage potentials of murine lymphoid progenitors. Blood *117*, 2618–2624.

Rothenberg, E.V. (2007). Negotiation of the T lineage fate decision by transcription-factor interplay and microenvironmental signals. Immunity *26*, 690–702.

Rybtsov, S., Sobiesiak, M., Taoudi, S., Souilhol, C., Senserrich, J., Liakhovitskaia, A., Ivanovs, A., Frampton, J., Zhao, S., and Medvinsky, A. (2011). Hierarchical organization and early hematopoietic specification of the developing HSC lineage in the AGM region. J. Exp. Med. *208*, 1305–1315.

Schlenner, S.M., and Rodewald, H.R. (2010). Early T cell development and the pitfalls of potential. Trends Immunol. *31*, 303–310.

Schlenner, S.M., Madan, V., Busch, K., Tietz, A., Läufle, C., Costa, C., Blum, C., Fehling, H.J., and Rodewald, H.R. (2010). Fate mapping reveals separate origins of T cells and myeloid lineages in the thymus. Immunity *32*, 426–436.

Schulz, C., Gomez Perdiguero, E., Chorro, L., Szabo-Rogers, H., Cagnard, N., Kierdorf, K., Prinz, M., Wu, B., Jacobsen, S.E., Pollard, J.W., et al. (2012). A lineage of myeloid cells independent of Myb and hematopoietic stem cells. Science *336*, 86–90.

Seita, J., and Weissman, I.L. (2010). Hematopoietic stem cell: self-renewal versus differentiation. Wiley Interdiscip Rev Syst Biol Med *2*, 640–653.

Sitnicka, E., Brakebusch, C., Martensson, I.L., Svensson, M., Agace, W.W., Sigvardsson, M., Buza-Vidas, N., Bryder, D., Cilio, C.M., Ahlenius, H., et al. (2003). Complementary signaling through flt3 and interleukin-7 receptor alpha is indispensable for fetal and adult B cell genesis. J. Exp. Med. *198*, 1495–1506.

Solar, G.P., Kerr, W.G., Zeigler, F.C., Hess, D., Donahue, C., de Sauvage, F.J., and Eaton, D.L. (1998). Role of c-mpl in early hematopoiesis. Blood *92*, 4–10.

Welner, R.S., Esplin, B.L., Garrett, K.P., Pelayo, R., Luche, H., Fehling, H.J., and Kincade, P.W. (2009). Asynchronous RAG-1 expression during B lymphopoiesis. J. Immunol. *183*, 7768–7777.

Ye, M., and Graf, T. (2007). Early decisions in lymphoid development. Curr. Opin. Immunol. *19*, 123–128.

Yokota, T., Huang, J., Tavian, M., Nagai, Y., Hirose, J., Zúñiga-Pflücker, J.C., Péault, B., and Kincade, P.W. (2006). Tracing the first waves of lymphopoiesis in mice. Development *133*, 2041–2051.

Yoshimoto, M., Montecino-Rodriguez, E., Ferkowicz, M.J., Porayette, P., Shelley, W.C., Conway, S.J., Dorshkind, K., and Yoder, M.C. (2011). Embryonic day 9 yolk sac and intra-embryonic hemogenic endothelium independently generate a B-1 and marginal zone progenitor lacking B-2 potential. Proc. Natl. Acad. Sci. USA *108*, 1468–1473.

Yoshimoto, M., Porayette, P., Glosson, N.L., Conway, S.J., Carlesso, N., Cardoso, A.A., Kaplan, M.H., and Yoder, M.C. (2012). Autonomous murine T-cell progenitor production in the extra-embryonic yolk sac before HSC emergence. Blood *119*, 5706–5714.

Yuan, J., Nguyen, C.K., Liu, X., Kanellopoulou, C., and Muljo, S.A. (2012). Lin28b reprograms adult bone marrow hematopoietic progenitors to mediate fetal-like lymphopoiesis. Science *335*, 1195–1200.